MR assessment of radiation-induced blood-brain barrier permeability changes in rat glioma model.

W G Krueck, U P Schmiedl, K R Maravilla, A M Spence, F L Starr and J Kenney

AJNR Am J Neuroradiol 1994, 15 (4) 625-632
http://www.ajnr.org/content/15/4/625

MR Assessment of Radiation-Induced Blood-Brain Barrier Permeability Changes in a Rat Glioma Model

Wolfgang G. Krueck, Udo P. Schmiedl, Kenneth R. Maravilla, Alexander M. Spence, Frank L. Starr, and James Kenney

PURPOSE: To assess the potential of a T1-weighted, gadolinium-enhanced MR technique for quantifying radiation-induced changes of blood-brain barrier permeability in a model of stereotactically implanted intracerebral gliomas in rats. **METHODS:** We calculated the gadolinium blood-to-tissue transport coefficient for gadopentetate dimeglumine from signal intensities in sequential MR images in nine control animals that were not irradiated and in five and three animals that had received 2500 cGy and 1500 cGy whole-brain irradiation, respectively, at 2 days before imaging. **RESULTS:** The average blood-to-tissue transport coefficient values were 9.76 $mL \cdot kg^{-1} \cdot min^{-1}$ in the control group, 23.41 $mL \cdot kg^{-1} \cdot min^{-1}$ in the 2500-cGy group, and 25.63 $mL \cdot kg^{-1} \cdot min^{-1}$ in the 1500-cGy group. Blood-to-tissue transport coefficients were significantly higher after irradiation, indicating increased radiation-induced blood-brain barrier permeability. Similar increased blood-brain barrier leakiness in brain tumors after high-dose irradiation has been shown by previous nuclear medicine studies using quantitative autoradiography. **CONCLUSION:** Contrast-enhanced dynamic MR of brain gliomas is a sensitive method to document radiation-induced blood-brain barrier breakdown. Quantitative gadolinium-enhanced MR may become a useful tool for the management of patients with brain tumors undergoing radiation therapy.

Index terms: Blood-brain barrier; Brain, effects of irradiation on; Brain, magnetic resonance; Brain neoplasms, therapeutic radiology; Glioma; Animal studies

AJNR Am J Neuroradiol 15:625–632, Apr 1994

The concept of the blood-brain barrier is based on the observation that many substances present in blood plasma cannot enter the brain parenchyma. Layers of endothelial cells sealed by tight junctions and of arachnoidal or choroidal cells are the physical component of this barrier. However, facilitated diffusion and active transport mechanisms involving pinocytotic vesicles allow substances such as glucose and amino acids to diffuse from the luminal to the abluminal side of the vessel wall, while other molecules of similar size remain confined to the intravascular space (1, 2). Both a greater than normal pinocytotic cell activity and widening of tight junctions cause increased blood-brain barrier permeability in the dysfunctional capillary endothelium of malignant gliomas (3, 4, 5). Positron emission tomography has been used to quantitate altered blood-brain barrier permeability in human and rat astrocytic gliomas (1, 2, 6–9). Alternatively, magnetic resonance (MR) imaging has proved useful for monitoring increased blood-brain barrier permeability in nonirradiated human and rat brain tumors (9–12). MR imaging has also been a sensitive tool in establishing molecular size–dependent permeability of tumor blood-brain barrier to different contrast media (13). In the current study we focused on the MR quantitation of radiation-induced permeability changes in implanted gliomas in rats. The blood-to-tissue transport coefficient was calculated for gadopentetate dimeglumine using a graphic approach as a measure to quantitate capillary permeability in irradiated and nonirradiated gliomas (12). We expected to establish an imaging tool useful to quantitate

Received March 9, 1993; accepted pending revision June 1; revision received January 6, 1994.

From the Departments of Radiology (W.G.K., U.P.S., K.R.M. F.L.S., J.K.) and Neurology (A.M.S.), University of Washington School of Medicine, Seattle; and Department of Radiation Oncology (W.G.K.), University of Tuebingen School of Medicine, Tuebingen, Germany.

W. Krueck is a postdoctoral fellow supported by the Deutsche Forschungsgemeinschaft, Bonn, Germany.

Address reprint requests to Udo P. Schmiedl, MD, PhD, Department of Radiology, University of Washington, School of Medicine, SB-05, Seattle, WA 98195.

AJNR 15:625–632, Apr 1994 0195-6108/94/1504–0625

radiation-induced changes of blood-brain barrier permeability.

Materials and Methods

Overview

In our experiment we used glioma-bearing control rats (n = 9) and rats with gliomas irradiated with 1500 cGy (n = 3) and 2500 cGy (n = 5), respectively. All rats were examined on day 16 after tumor implantation using gadolinium-enhanced T1-weighted MR. Irradiated rats had received whole-brain irradiation 2 days before the imaging experiment. A conversion factor for translating enhancement into calculated tissue gadolinium concentrations was derived by analyzing the frozen tumors of 11 rats and their last respective enhancement. Tissue gadolinium concentrations were calculated for all measurements obtained on all the tumors. The capillary permeability coefficient K_i was then calculated for each rat.

Animal Model

Astrocytic 36B-10 glioma cells, a nitrosurea-induced cell line, were stereotactically implanted into the right cerebral hemispheres of male F-344 rats (160–220 g each) following a previously described technique (14–17). The stereotactic coordinates were: 6 mm deep, 3 mm to the right of midline, and 6 mm anterior to the frontal plane (14, 18). All animals developed gliomas. A total of 17 rats received tumor implants and were divided into control (not receiving irradiation) and treatment groups. The control group contained nine animals; the 1500-cGy group, three anímals; and the 2500-cGy group, five animals. Radiation was performed 14 days after tumor implantation; irradiated animals and nonirradiated rats were imaged at 16 days after tumor implantation. Thus, radiation effects on blood-brain barrier permeability were measured 2 days after radiation treatment. Time intervals were chosen based on previous work using quantitative autoradiography to measure K_i in the identical model (17). Three of the six animals originally designated to be examined after receiving 1500 cGy had died before they could be imaged. For technical reasons we decided not to pursue the hypothesis that there might be a difference between the mean coefficients of rats irradiated with 1500 and 2500 cGy.

Radiotherapy

High-energy gamma radiation was delivered to the anesthetized animals (25 mg/kg pentobarbital intraperitoneally) in single doses of 1500 (n = 3) or 2500 (n = 5) cGy, via equally weighted, parallel opposing lateral ports, at a dose rate of 145 cGy/min using a Shepard cesium-137 therapy unit (660 keV). The source-midbrain distance was 32 cm. The animals were shielded by a 2.5-cm layer of Lipowitz metal, except for the neurocranium and the eyes. Dosimetry was carried out using a Farmer ionization chamber.

Single-dose radiation was chosen, because permeability results obtained were to be compared with results obtained in the identical model with quantitative autoradiography reported previously (17). In this study, radiation was given at a single dose of 2000 cGy, and permeability was measured 1 and 2 days after radiation. We chose doses of 15 Gy and 25 Gy that were in the neighborhood of the previously studied dose, so results were comparable. We also wondered whether we could possibly detect a dose response after 15 and 25 Gy radiation. For the reasons previously stated this proved not to be possible.

The rationale for measuring blood-brain barrier permeability 2 days after irradiation was that a previous study (17) had shown that after an initial decrease on day 1, blood-brain barrier permeability would increase over baseline at 48 hours after treatment. Also, rats implanted with glioma cells have a limited life span, about 21 days after implantation. Tumors reach a reasonable size for imaging approximately 14 to 16 days after implantation. Given these time constrictions, we could reasonably study only one time point after radiation. We realize that this does not in any way reflect clinical practice. The purpose of this study was rather to investigate whether radiation-induced permeability changes can be measured with contrast-enhanced MR.

MR Technique

Before imaging, a 25-gauge butterfly needle was inserted into the tail vein and PE 10 tubing was implanted in the left femoral artery of the anesthetized rats. Tail vein catheters used for contrast media injection and arterial catheters used for blood sampling were accessible from outside the magnet bore, allowing simultaneous contrast media injection and sequential blood sampling during MR experiments.

A 1.5-T clinical system (Signa, General Electric, Milwaukee, Wis) was used. The anesthetized animals were placed in a 10-cm inner diameter wrist coil. The animals' heads were imaged in the supine position, using an axial T1-weighted spin-echo sequence (CSMEMP, 233/21/4 [repetition time/echo time/excitations]). An 8-cm field of view, a section thickness of 3 mm, and a 256 × 128 matrix were used, yielding an in-plane resolution of 0.3 × 0.6 mm.

Blood Sampling, Contrast Injection, and Image Acquisition

Slow intravenous infusion of contrast at a total dose of 0.3 mmol/kg was carried out over approximately 20 minutes. Arterial blood samples (volume = 0.2 mL each) were drawn before and at 2- to 3-min intervals during contrast infusion. Blood samples were obtained simultaneously with each MR acquisition. After each blood sample an identical volume of heparinized saline was administered to the rat. Diluted gadopentetate dimeglumine (Magnevist, Berlex, Wayne, NJ; 0.15 mol/L) was continuously injected at a rate of approximately 0.025 mL/min via the animals' tail veins. The start of contrast injection was defined as time 0. Contrast injection, image acquisition, and blood sampling

were continued for 20 minutes. The number of measurements obtained for each rat is shown in the Table. Immediately after the acquisition of the last image, the rats were killed by intravenous administration of a pentobarbital overdose. The brains of all rats were quickly removed and frozen in liquid nitrogen. Excised tumors were stored deep-frozen for quantitative gadolinium analysis using inductively coupled plasma atomic emission spectroscopy. Only brain samples in which the tumors could be easily separated from the normal brain tissue, meninges, and skull were used for inductively coupled plasma atomic emission spectroscopy gadolinium determination (n = 11).

Analysis of MR Images

To measure signal enhancement, regions of interest were placed over the area of the intraaxial tumor and over the central medulla of the non–tumor-bearing, opposite brain hemispheres. Diameters of regions of interest ranged from 3 to 8 mm, depending on tumor size. Regions of interest of identical size and shape were examined in identical locations. Region of interest intensity values were normalized to an external standard containing gadopentetate dimeglumine. We calculated signal enhancement as the fractional increase in signal intensity of the postcontrast over to the precontrast image in decimal fractions of 1.

Enhancement was calculated using the formula:

$$E = [(I(t)_{tu} - I(t)_{ph}) - (I(0)_{tu} - I(0)_{ph})]/(I(t)_{tu} - I(t)_{ph})$$

where E is enhancement (dimensionless, arbitrary units); $I(0)_{tu}$ is average region of interest signal intensity (arbitrary units) over the tumor region at the start of the gadolinium infusion; $I(t)_{tu}$ is average region-of-interest signal intensity (arbitrary units) over the tumor region at time t of the gadolinium infusion; $I(0)_{ph}$ is average region-of-interest signal intensity (arbitrary units) over the phantom at the start of the gadolinium infusion; and $I(t)_{ph}$ is average region-of-interest signal intensity (arbitrary units) over the phantom at time t of the gadolinium infusion.

Plasma Gadolinium Measurement

Blood plasma samples were diluted in distilled water; gadolinium concentration was measured by inductively coupled plasma atomic emission spectroscopy. Calibration of the unit was performed using 0- to 20-parts per million dilutions of 1000 parts per million gadolinium standard solution (Aldrich, Milwaukee, Wis). The sensitivity of this method for gadolinium determination is 17 parts per billion.

Quantitation of Blood-to-Tissue Transport

To quantitate blood-brain barrier permeability, we calculated the blood-to-tissue transport coefficient, K_i, using the graphical method of Patlak et al (19). The increase of the tissue gadolinium concentration (A_t) over time (t) is expressed by:

$$1) \qquad dA_t/dt = K_i\, C_{pt} + V_i\, dC_{pt}/dt,$$

where C_{pt} is plasma gadolinium at time t, and V_i is plasma volume per unit mass of tissue plus the volume of any space for which exchange with the intravascular space is rapid. Tissue gadolinium at time t is described by:

$$2) \qquad A_t = K_i \int_0^t C_{pt'}dt' + V_i\, C_{pt},$$

hence:

$$3) \qquad A_t/C_{pt} = K_i \int_0^t C_{pt'}dt'/C_{pt} + V_i.$$

On a plot of A_t/C_{pt} versus $\int_0^t C_{pt'}dt'/C_{pt}$, K_i is calculated as the slope of the regression curve. The Y intercept (V_i) of this curve theoretically represents the plasma volume per unit mass of tissue plus the combined volume of tertiary spaces for which the exchange of gadolinium with the plasma is rapid (12, 14, 19).

Average K_i's, correlation coefficients, confidence intervals, and number of data points used for graphical analysis

Rat	Radiation Dose (Gy)	K_i (ml/kg/min)	95% Confidence Interval	Correlation Coefficient	Number of Points	Y Intercept
1	0	3.58	0.88–6.28	0.97	11	−5.77
2	0	6.49	1.37–11.59	0.87	9	23.49
3	0	7.61	−24.62–39.84	0.99	3	−1.05
4	0	8.85	2.26–18.61	0.65	11	153.86
5	0	10.37	2.40–18.34	0.99	10	13.35
6	0	11.12	19.50–2.73	0.97	11	11.47
7	0	12.19	2.82–21.55	0.96	10	24.66
8	0	12.36	3.04–21.67	0.95	11	32.10
9	0	15.22	−0.75–31.18	0.99	6	54.00
10	15	1.79	0.44–3.14	0.99	11	6.57
11	15	29.22	2.18–56.26	0.88	6	52.30
12	15	45.88	−2.78–95.54	0.95	5	39.43
13	25	10.92	2.31–19.52	0.98	11	17.05
14	25	13.56	2.03–29.15	0.94	7	19.24
15	25	29.41	6.22–52.59	0.96	9	25.87
16	25	30.00	−1.81–61.81	0.93	5	22.23
17	25	33.16	7.02–59.30	0.97	9	1.79

Statistics

To assess the significance of differences of group means of K_i's we used two-tailed *t* testing assuming unequal variances of our test groups. Thus we tested Welch *t* (reasonably independent of group variances) against Student *t* as the critical value for $P < .05$ (28). K_i values were determined from graphs of A_t/C_{pt} by least squares regression. Confidence intervals for K_i's were calculated multiplying the regression standard errors by the critical values of $t_{0.05(2),n-2}$ ($P < .05$; n = number of points used).

Results

Correlation of Enhancement to Gadolinium Concentration in Tumor Tissue

Figure 1 shows a graph of tissue gadolinium concentrations versus MR signal enhancement of the tumors (n = 11). The gadolinium concentrations found in tumor tissue varied from 20.67 to 494.83 μmol/kg. Using least squares regression through the origin, a calibration factor was calculated to predict tumor gadolinium concentration (A_t) as a linear function of tumor enhancement (E):

4) $$A_t = 123 \times E.$$

The correlation coefficient for equation 4 is 95.39%. The 95% confidence intervals for tissue gadolinium predicted using equation 4 were ±23%, calculated using the standard equations for confidence interval regression coefficients from linear regression through the origin.

Blood-to-Tissue Transport Coefficient Tumor Tissue

There was no visible enhancement as a sign of major contrast leakage from capillaries in normal brain tissue in any of the irradiated or control animals. Enhancement values in 13 of 17 did not exceed 0.1 in the nontumorous areas over which the regions of interest had been placed, varying from 0.01 to 0.16 (in one rat irradiated with 2500 cGy), all below safe detection limits. Because of the small number of animals examined, we could not detect a significant difference in behavior of enhancement values of irradiated and nonirradiated nontumorous brain matter.

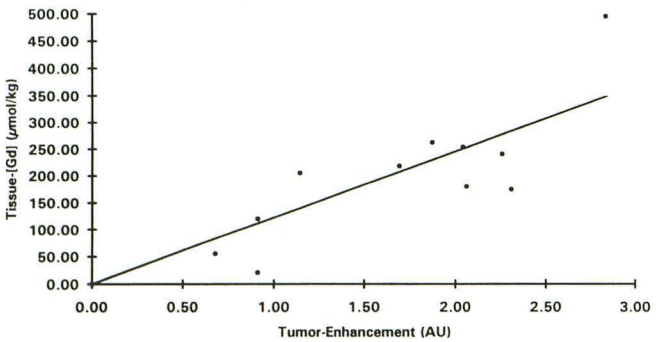

Fig. 1. Calibration plot of tumor gadolinium (A_t) over enhancement (E). The calibration factor is $A_t = 123 \times E$. The correlation coefficient is 95.4%. The 95% confidence intervals for tissue gadolinium predicted using the calibration factor are ±23%. AU indicates arbitrary units without dimension.

Both irradiated and nonirradiated tumors showed visible enhancement during intravenous infusion of gadolinium. MR images demonstrating the time course of tumor enhancement in rat 15 after 2500-cGy whole brain irradiation are shown in Figure 2. Figure 3 shows the graphical analysis of measurements obtained in rat 15. Figure 3A shows tumor enhancement and plasma gadolinium versus time as measure in this rat (number 15). For the same rat, calculated tumor gadolinium versus time is shown in Figure 3B. The calculation of K_i as the slope of A_t/C_{pt} versus ${}_0^t\int C_{pt}\cdot dt'/C_{pt}$ is demonstrated in Figure 3C. K_i for this instance is 29.41 $mL\cdot kg^{-1}\cdot min^{-1}$.

Curves of A_t/C_{pt} versus ${}_0^t\int C_{pt}\cdot dt'/C_{pt}$ were nearly linear over the whole infusion time in all nonirradiated animals. Curves of three out of eight irradiated animals (rats 11, 12, and 16) were only linear in their initial portions, representing 8 to 10 minutes of infusion time. K_i's were calculated in all rats using the linear portion of the curve.

K_i values (slopes) and K_i confidence intervals (basing on slope variance), as well as the Y intercepts of the linear portions of plots of A_t/C_{pt} versus ${}_0^t\int C_{pt}\cdot dt'/C_{pt}$ are presented in the Table. K_i values ranged from 3.58 to 15.22 $mL\cdot kg^{-1}\cdot min^{-1}$ (average = 9.76) in the control group (n = 9), from 10.92 to 33.16 $\cdot kg^{-1}\cdot min^{-1}$ (average = 23.41) in the group that had received 2500 cGy (n = 5), and from 1.79 to 45.88 $mL\cdot kg^{-1}\cdot min^{-1}$ (average 25.63) in the group irradiated with 1500 cGy (n = 3) (Fig 4). The Y intercepts for K_i values varied, ranging from −5.77 to 153.86 mL/kg.

Discussion

In the present investigation we showed the usefulness of gadolinium-enhanced, T1-weighted MR studies in measuring radiation-induced blood-brain barrier permeability changes in malignant gliomas.

Irradiation with 1500 to 2500 cGy caused a significant increase in the gadopentetate dimeglu-

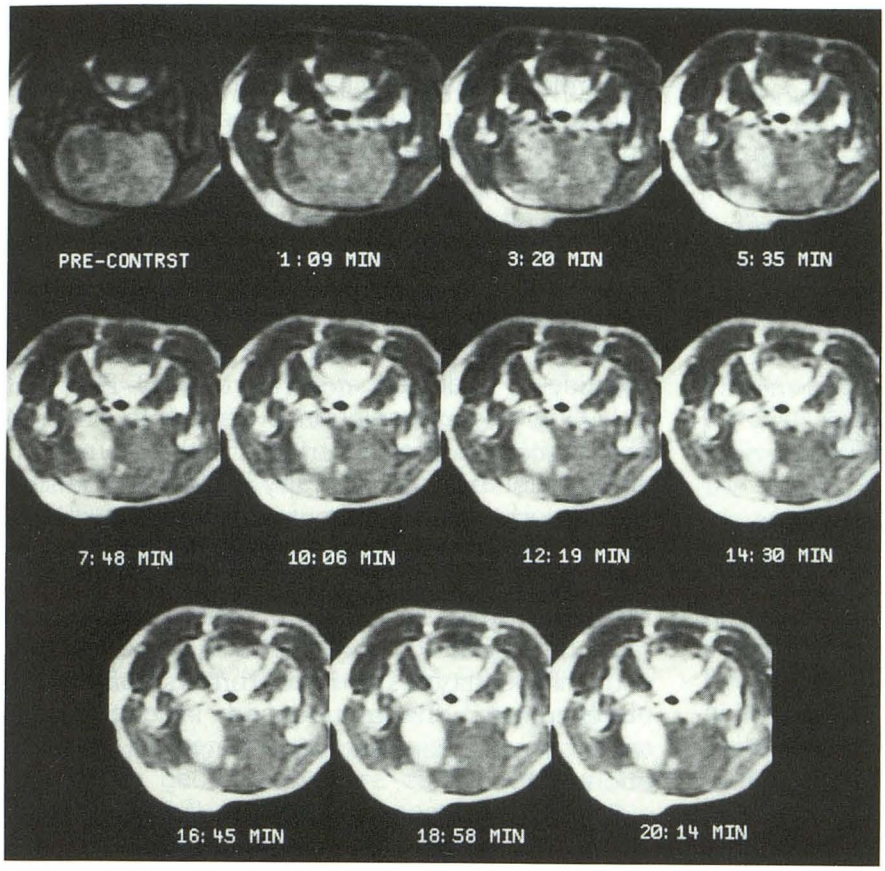

Fig. 2. Sequential MR images demonstrating the time course of tumor enhancement in rat 15 at 48 hours after 2500 cGy whole brain irradiation.

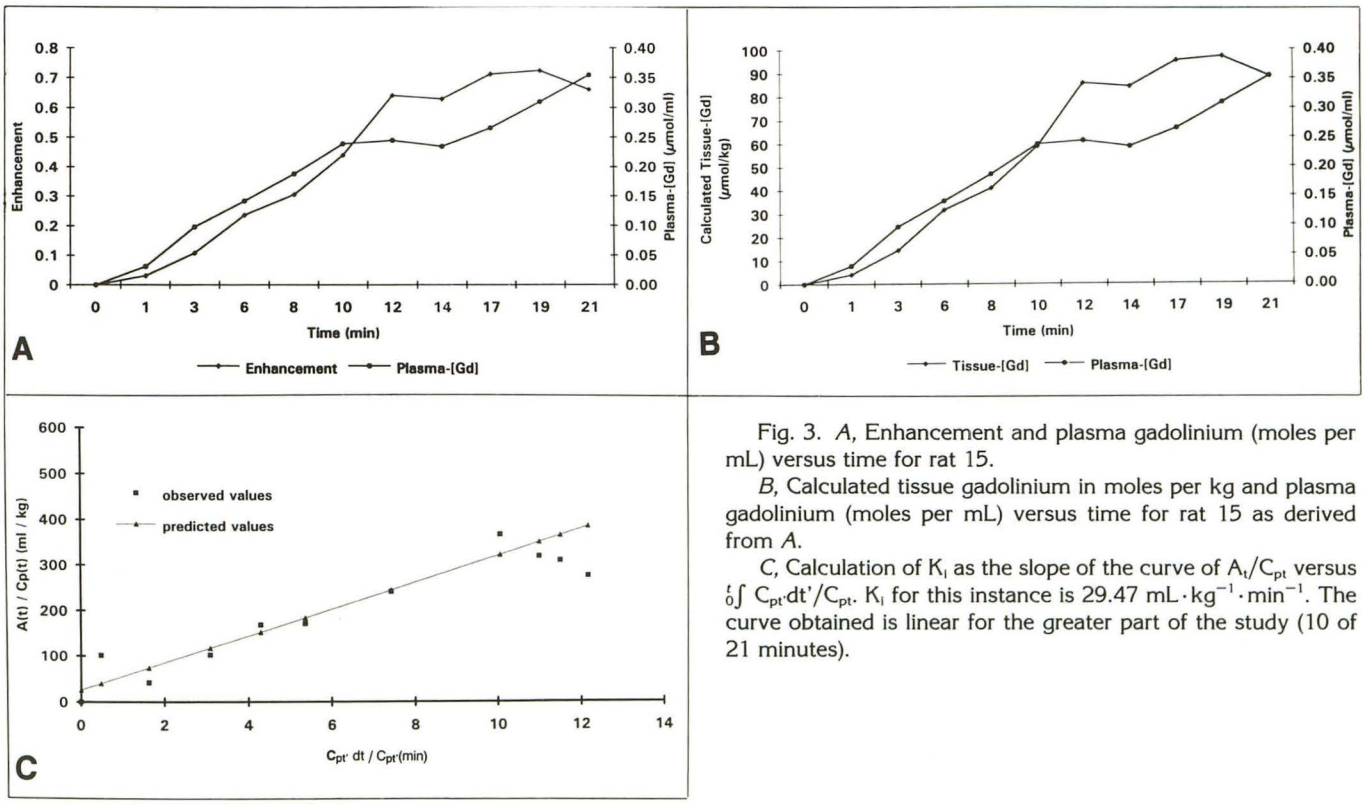

Fig. 3. *A*, Enhancement and plasma gadolinium (moles per mL) versus time for rat 15.

B, Calculated tissue gadolinium in moles per kg and plasma gadolinium (moles per mL) versus time for rat 15 as derived from *A*.

C, Calculation of K_i as the slope of the curve of A_t/C_{pt} versus $\int_0^t C_{pt} \cdot dt' / C_{pt}$. K_i for this instance is 29.47 $mL \cdot kg^{-1} \cdot min^{-1}$. The curve obtained is linear for the greater part of the study (10 of 21 minutes).

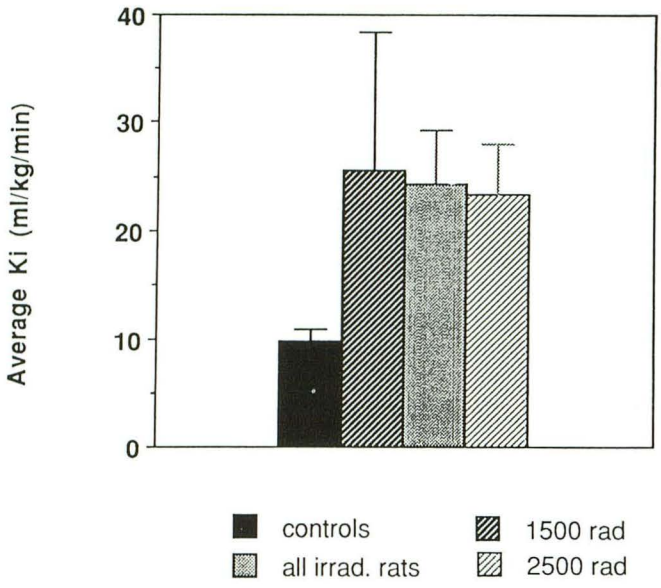

Fig. 4. Average K_i values +1 SE of control (n = 9) and rats that received 1500 cGy (n = 3) and 2500 cGy (n = 5).

mine blood-to-tissue transport constant in gliomas 2 days after irradiation, demonstrating greater vascular permeability than the control. Inspection of the excised tumors showed solid tumors of whitish color without gross necrosis or hemorrhage 48 hours after irradiation, a finding previously described by Spence et al (17). Using quantitative autoradiography with ^{125}I-amino-isobutyric acid, they reported a decrease in K_i on day 1 after irradiation with 2000 cGy and a return to approximately the preirradiation levels 2 days after irradiation (17). Our finding of increased tumor capillary leakiness after radiation appears therefore to be somewhat contradictory to the results obtained by quantitative autoradiography using the same tumor model. Although variability in tumor growth and response to radiation may account for part of the discrepancy, differences in technique are likely more important. The most important difference between the two studies is the lower radiation dose used by Spence et al and the earlier time point after radiation at which permeability was measured. Although the exact mechanism of the relatively decreased permeability in tumors measured 24 hours after radiation with 2000 cGy is not exactly understood, radiation could cause endothelial cells to flatten and swell, thus narrowing the spaces between cells. This process, which may be rapidly reversible, could contribute to the decrease in K_i early after radiation followed by increased permeability at 2 days as measured by Spence at al and in the current paper. Furthermore, the postirradiation values of K_i reported by Spence et al are results of an endpoint study that did not monitor the dynamics of transcapillary transport in the time course of an infusion experiment and may be limited in instances where capillaries are highly permeable to the tracer used (17).

Song et al, in subcutaneously implanted Walker-256 tumors, reported an increase of ^{125}I-serum albumin extravasation 2 days after irradiation with 2000 cGy, along with a decrease in intravascular blood volumes as determined using creatine-151–labeled erythrocytes (20–22). Not only single-dose irradiation experiments, but also observations in patients treated with conventionally fractionated radiotherapy by Qin et al, using technetium-99m glucoheptonate emission computed tomography, were able to show significant increases in pixel counts over the tumor regions ranging from 6% to 107% after fractionated radiotherapy of 30 to 40 Gy in 10 of 14 patients with different types of brain tumors. Data were obtained from the unirradiated, irradiated, and tumor areas before and after fractionated irradiation (23).

The above-mentioned experimental and clinical results were acquired in studies technically different from ours. However, they corroborate our findings of increased capillary permeability in brain tumors at 2 days after radiation therapy. Capillary permeability changes measured by standard methods such as quantitative autoradiography in untreated brain tumors and in gliomas after single-dose radiotherapy were in the range of the values we obtained using contrast-enhanced spin-echo MR. The average K_i for nonirradiated gliomas reported using quantitative autoradiography (11 $mL \cdot kg^{-1} \cdot min^{-1}$) is not significantly different from the mean K_i for gadolinium we found in nonirradiated control animals (9.75 $mL \cdot kg^{-1} \cdot min^{-1}$) (17). The average K_i measured for nonirradiated rats in this study also corresponds well to the K_i reported previously (9.2 $mL \cdot kg^{-1} \cdot min^{-1}$) for the same tumors studied with MR between 13 and 18 days after implantation, confirming the reproducibility of the method presented here (12). It seems legitimate to argue that contrast-enhanced spin-echo MR is a reliable technique for detecting blood-brain barrier alterations induced in brain tumors by experimental irradiation. MR may also be an appropriate method for monitoring similar changes in brain tumors of patients treated with conventionally fractionated radiotherapy.

Our study did not specifically address the question of local vascular blood volume. However, some of the above-mentioned data clearly show that in the first days after high-dose, single fraction irradiation local blood flow has a tendency to decrease, most probably because of swelling of endothelial cells. Changes in local perfusion thus probably were no major cause of increased enhancement in irradiated tumors.

The role of the transcapillary transport constant, K_i, and of a number of other parameters involved in the diffusion of drugs across the blood-brain barrier was demonstrated in several radionuclide studies that examined blood-brain barrier changes in unirradiated brain tumors (6, 24, 25, 19). K_i can be used as a reliable estimate of the permeability–surface-area product (PS) given that the extraction fraction ($E = K_i/F \times V_c$; F = regional blood flow; V_c = capillary volume/unit mass of tissue) is smaller than 0.1.

Calculation of K_i is based on the correlation between tissue enhancement and tissue gadolinium, and spectrometric measurement of plasma and tissue gadolinium were carried out in this project (12, 13). In the recent past several authors have also used contrast-enhanced MR in assessing changes in blood-brain barrier permeability in both brain tumors and lesions caused by multiple sclerosis (9, 10, 11, 26, 27). Different MR approaches were chosen to measure transcapillary transport of gadopentetate dimeglumine. Larsson et al, assuming a linear relationship between 1/T1 and tissue gadolinium, calculated blood-brain barrier permeability changes in brain lesions on the basis of an estimate of the unknown distribution volume (V_d) of gadopentetate dimeglumine (11). Susceptibility-induced changes in signal-time curves of a T2*-weighted fast low-angle shot sequence were used by Perman et al to calculate tissue gadolinium concentration of brain tissue (11). Yet, the influence of pulsatile arterial flow, spatial resolution, and the sampling rate on the accuracy of the calculated input function could not be determined.

Nonlinear portions of curves of A_t/C_{pt} versus ${}_0^t\int C_{pt'}dt'/C_{pt}$ during the later phases of the infusion may represent significant backflux of tracer and/or contrast from the extravascular space into the intravascular compartment as discussed by others (8, 13, 19, 24). Three (37.5%) of the animals irradiated in this study showed nonlinear enhancement slopes later than 10 min after start of the infusion. In these instances, K_i's were calculated using the linear portions of curves of A_t/C_{pt} versus ${}_0^t\int C_{pt'}dt'/C_{pt}$. Because comparable nonlinear portions did not appear in the curves of nonirradiated control animals, marked nonlinearity of contrast enhancement over time may be another indicator of increased blood-brain barrier permeability.

Our data do not reveal a relationship between blood-brain barrier changes and different radiation doses as described by Quin et al in a study of fractionated radiation therapy in humans (23). These findings are in agreement with the observations of Spence et al (17). In the present study, as well as in the study of Spence et al, single high-dose irradiation was applied 48 hours before the experiments, whereas fractionated doses obviously were used in human patients. Thus, the apparent discrepancy may be explained by, among other factors, a stronger repair component and vascular recovery resulting in a relatively smaller increase in blood-brain barrier permeability after fractionated radiotherapy.

The use of gadolinium-enhanced MR to quantitate radiation effects on capillary permeability as shown in this paper does require measurement of the arterial input function and tissue gadolinium. Although the relationship between measured enhancement and tissue gadolinium established for the animal model will likely be applicable to humans—provided identical MR parameters are used—the arterial input function will vary among individuals, depending on cardiac output, intravascular volume, and injection technique. Further laboratory and patient studies are needed to develop a noninvasive method of calculating the arterial input function and obviate the measurement of arterial gadolinium. Additional factors that will have to be addressed in this work include the influence of spatial resolution, arterial flow, sampling rate, and susceptibility effects on the MR signal before this approach could be implemented as a routine clinical tool.

T1-weighted, gadolinium-enhanced spin-echo imaging with simultaneous measurement of arterial gadolinium is able to monitor reliably blood-brain barrier permeability changes in the time course of brain tumor radiotherapy. Changes in radiation-induced capillary permeability may be important to define better the appropriate starting point for chemotherapy within a combined treatment scheme to permit optimal drug penetration into the tumor tissue in individual patients. Furthermore, the response of tumor to radiation and chemotherapy may be monitored more closely. This may eventually lead to further optimization

of radiation fractionation schemes and development of improved tumor treatment protocols.

In summary, the results of this work demonstrate the potential of gadolinium-enhanced, T1-weighted MR imaging as an accurate method in detecting and quantifying radiation-induced blood-brain barrier changes in irradiated gliomas. The present data are in good agreement with previous experiments using AIB-autoradiography, positron emission tomography, and emission computed tomography, methods that have been recognized as standard approaches in measuring blood-brain barrier function. Quantitative gadolinium-enhanced MR may become a useful tool for the treatment of patients with brain tumors undergoing radiation therapy.

Acknowledgments

We thank Janet Rasey, PhD, for her collaboration, Lay Chin, RT, for his technical assistance in establishing dosimetry and irradiation technique, and Donna Stein for her important efforts in tumor cell preparation and care.

References

1. Bradbury M. *The concept of the blood-brain-barrier.* Chichester: Wiley, 1979
2. Christensen HN, Liang M, Archer EG. A distinct Na^+-requiring transport system for alanine, serine, and cysteine, and similar amino acids. *J Biol Chem* 1967;242:5237–5246
3. Kohn S, Front D, Nir I. Blood-brain barrier permeability of human gliomas as determined by quantitation of cytoplasmic vesicles of the capillary endothelium and scintigraphic findings. *Cancer Invest* 1989;7:313–321
4. Nir I, Levanon D, Iosilevsky G. Permeability of blood vessels in experimental gliomas: uptake of 99 mTc-glucoheptonate and alteration in blood-brain barrier as determined by cytochemistry and electron microscopy. *Neurosurgery* 1989;25:523–531
5. Wolff M, Boker DK. Immunohistochemical demonstration of immunoglobulins and albumin in human brain tumors. *Clin Neuropathol* 1989;8:72–78
6. Groothuis DR, Molnar P, Blasberg RG. Regional blood flow and blood-to-tissue-transport in five brain tumor models. *Prog Exp Tumor Res* 1984;27:132–153
7. Hawkins RA, Phelps M, Huang SC, et al. Kinetic evaluation of blood-brain-barrier permeability in human brain tumors with [^{68}Ga]-EDTA and positron computed topography. *J Cereb Blood Flow Metab* 1984;4:507–515
8. Ianotti F, Fieschi C, Alfano B, et al. Simplified, non-invasive measurement of Blood-Brain-Barrier Permeability. *J Comput Assist Tomogr* 1987;11:390–397
9. Bullock PR, Mansfield P, Gowland P, Worthington BS, Firth JL. Dynamic imaging of contrast enhancement in brain tumors. *Magn Reson Med* 1991;19:293–298
10. Larsson H, Stubgaard M, Fredriksen J, Jensen M, Henriksen O, Paulson O. Quantitation of blood-brain-barrier defects by magnetic resonance imaging and Gadolinium-DTPA in patients with multiple sclerosis and brain tumors. *Magn Reson Med* 1990;16:117–131
11. Perman WH, Gado MH, Larson KB, Perlmutter JS. Simultaneous MR acquisition of arterial and brain signal-time curves. *Magn Reson Med* 1992;28:74–83
12. Kenney J, Schmiedl UP, Maravilla KR, et al. Measurement of blood-brain-barrier permeability in a tumor model using magnetic resonance imaging with gadolinium-DTPA. *Magn Reson Med* 1992;27:68–75
13. Schmiedl UP, Kenney J, Maravilla KR. Dyke award paper. Kinetics of pathologic blood-brain-barrier permeability in an astrocytic glioma using contrast-enhanced MR. *AJNR Am J Neuroradiol* 1992;13:5–14
14. Barker M, Hoshino T, Gurcay O, Nielsen SL, Downie R, Eliason J. Development of an animal brain tumor model and its response to therapy with 1,3-bis(2-chloroethyl)-1-nitrosourea. *Cancer Res* 1973;33:976–986
15. Spence AM, Coates PW. Scanning and transmission electron microsopy of cloned rat astrocytoma cells treated with dibutyryl cyclic AMP in vitro. *J Cancer Res Clin Oncol* 1981;100:51–58
16. Spence AM, Coates PW. Scanning electron microscopy of cloned astrocytic lines derived from ethylnitrosourea-induced rat gliomas. *Virchows Arch [B]* 1986;228:77–86
17. Spence AM, Graham MM, O'Gorman L, Muzi M, Abbot GL, Lewellen TK. Regional blood-to-tissue transport in an irradiated rat glioma model. *Radiat Res* 1987;111:225–236
18. Konig JFR, Klippel RA. *The rat brain: a stereotaxic atlas of the forebrain and lower parts of the brainstem.* Baltimore: Williams & Wilkins, 1963
19. Patlak CS, Fenstermacher J. Graphical evaluation of blood-to-brain transfer constants from multiple-time uptake data. *J Cereb Blood Flow Metab* 1983;3:1–7
20. Song CW, Levitt SH. Quantitative study of vascularity in Walker 256 carcinoma. *Cancer Res* 1971;31:587–589
21. Song CW, Payne JT, Levitt SH. Vascularity and blood flow in X-irradiated Walker carcinoma 256 of rats. *Radiology* 1973;108:429–434
22. Song CW, Payne JT, Levitt SH. Vascularity changes in Walker 256 carcinoma following X-irradiation. *Cancer Res* 1974;34:2344–2350
23. Qin DX, Zheng R, Tang J, Li JX, Hu YH. Influence of radiation on the Blood-Brain Barrier and optimum time of chemotherapy. *Int J Radiat Oncol Biol Phys* 1991;19:1507–1510
24. Blasberg RG, Molnar P, Groothuis D, Owens E, Fenstermacher J. Concurrent measurements of blood flow and transcapillary transport in avian sarcoma virus-induced experimental brain tumors: implications for chemotherapy. *J Pharm Exp Ther* 1984;231:724–735
25. Blasberg RG, Shapiro WR, Molnar P, Patlak CS, Fenstermacher JD. Local blood-to-tissue transport in Walker-256 metastatic brain tumors. *J Neurooncol* 1984;2:205–218
26. Tofts PS, Kermode AG. Measurement of the blood-brain barrier permeability and leakage space using dynamic MR imaging. 1. Fundamental concepts. *Magn Reson Med* 1991;17:357–367.
27. Yoshida K, Furuse M, Kaneoke Y, et al. Assessment of T1 time course changes and tissue-blood ratios after Gd-DTPA administration in brain tumors. *Magn Reson Imaging* 1989;7:9–15
28. Zar JH. Violations of the two-sample t test assumptions. In: Zar JH, ed. *Bio-statistical analysis.* 2nd ed. Englewood Cliffs: Prentice Hall, 1984:130–131